



1

2

3

4 **Changes in surface ozone in South Korea on diurnal to decadal time scale**  
5 **for the period of 2001-2021**

6

7 Si-Wan Kim<sup>1</sup>, Kyoung-Min Kim<sup>2</sup>, Yujoo Jeong<sup>1,2</sup>, Seunghwan Seo<sup>2</sup>, Yeonsu Park<sup>2</sup>, and  
8 Jeongyeon Kim<sup>2</sup>

9

10 <sup>1</sup>Irreversible Climate Change Research Center, Yonsei University, Seoul, South Korea

11 <sup>2</sup>Department of Atmospheric Sciences, Yonsei University, Seoul, South Korea

12

13

14

15 \*Corresponding author. E-mail: [siwan.kim@yonsei.ac.kr](mailto:siwan.kim@yonsei.ac.kr)

16

17

18

19

20 Short title: Ozone changes in South Korea

21

22



1

## Abstract

2 Increasing trends of tropospheric ozone in South Korea in the last decades have reported  
3 in several studies, based on various metrics. In this study, we derived the trends of surface  
4 ozone in South Korea utilizing the daily maximum 8-hours average ozone concentrations  
5 (MDA8) measured at the surface from 2001 to 2021 and analyzed diurnal, seasonal, multi-  
6 decadal variations of this parameter at city, province, and background sites. The 4<sup>th</sup> highest  
7 MDA8 values have positive trends at 7 cities and 8 provinces throughout 2001-2021 with  
8 approximately 1-2 ppb yr<sup>-1</sup> and were greater than 70 ppb after early 2010 for all sites,  
9 despite decreases of its precursor NO<sub>2</sub> and CO. The Seoul Metropolitan Area (SMA) and  
10 the background sites have different diurnal and seasonal characteristics of MDA8  
11 exceedances defined in this study (percentage of the data points with MDA8 > 70 ppb  
12 among all data points). SMA have much higher exceedances during summer than spring,  
13 while the background sites have much higher exceedances during spring than summer  
14 highlighting efficient local production of ozone in SMA during summer and strong  
15 influence of long-range transport during spring. The exceedances during spring and  
16 summer are similar for the rest of sites. The peaks of exceedances occur at 4-5 PM in SMA  
17 and most of locations, while exceedances mainly occur at 7-8 PM through night at the  
18 background sites. During spring of the COVID-19 pandemic (2020-2021), the MDA8  
19 ozone exceedances decreased for most of locations with large NO<sub>x</sub> reductions in South  
20 Korea and China compared to 2010-2019. The large decreases of the MDA8 ozone



1 exceedances occur in particular at the background sites during spring. In Gosung,  
2 Gangwondo (~600 m above sea level), the exceedances drop to ~5% from 30% in  
3 springtime during the COVID-19 pandemic. The concept of decreases of ozone in the  
4 boundary layer in Seoul and Gangwon-do to reductions in the emissions was confirmed by  
5 regional model simulations. The reductions of ozone exceedances did not occur at the  
6 major cities and provinces during summer of the COVID-19 pandemic with much smaller  
7 decreases of NO<sub>x</sub> in South Korea and China compared to spring. This study demonstrates  
8 distinctions between spring and summer in the formation and transport of surface ozone in  
9 South Korea and the need of monitoring and modeling with focus on different processes in  
10 each season or a finer time scale.



1 **1. Introduction**

2 Ozone in the low atmosphere (or troposphere) can be formed and accumulated by  
3 photochemical reactions involving nitrogen oxides and volatile organic compounds that  
4 emit from anthropogenic and natural sources (National Research Council, 1991; Monks et  
5 al., 2015). Ozone is an air pollutant harmful to public health and ecosystem and is a  
6 greenhouse gas warming the globe. Therefore, it is alarming that ozone concentrations near  
7 the surface and troposphere increase. Gaudel et al. (2018) reported rapidly increasing ozone  
8 trends from 2000 to 2014 in South Korea contrasting decreasing trends in North America  
9 and Europe utilizing available data from surface monitors, ozonesondes, and aircraft  
10 observations. Other studies also reported increasing ozone trends in South Korea for 2001-  
11 2018 (Lee et al., 2014; Shin et al., 2017; Lee et al., 2020; Yeo and Kim, 2021). Ozone in  
12 South Korea can be affected by ozone and its precursor in China. However, ozone data  
13 covering China were not included in Gaudel et al. (2018) because of lack of reported data.  
14 Recent studies highlighted rapidly increasing ozone trends in China from 2004 to 2020,  
15 particularly after 2013 (Li et al., 2019; Wang et al., 2020; Wang et al., 2022). Since the two  
16 countries are close enough to exchange ozone and its precursors, it would be essential to  
17 study the trends of ozone in South Korea associating with those in China. Particularly,  
18 spring and summer as warm season have different transport patterns and source-receptor



1 relationships relevant to surface and tropospheric ozone (e.g., Cooper et al., 2010).  
2 Therefore, it would be useful to investigate ozone trends in South Korea separately for  
3 spring and summer. There were large changes in atmospheric composition during the  
4 COVID-19 pandemic (Bauwens et al., 2020; Koo et al., 2020; Seo et al., 2021). The  
5 deviations caused by the pandemic from the long-term trends would provide a valuable  
6 perspective for planning of future environmental policy to improve ozone pollution. In this  
7 study, we characterize ozone trends and exceedances in South Korea from 2001 to 2021  
8 (including the COVID-19 period) focusing on the warm season, spring and summer.  
9 Diurnal, seasonal, and decadal changes at 7 cities, 8 provinces, and 3 background sites are  
10 studied. The causes for the large temporal changes are discussed based on regional model  
11 results.

12 The manuscript is organized as following. In section 2, the surface and satellite data,  
13 global and regional modeling, and other methods to utilize the data are explained. In section  
14 3, the results are summarized as long-term trends of ozone and its precursors,  
15 characteristics of diurnal variations, and spatiotemporal variations during the pandemic. In  
16 section 4, the regional model results based on various emission scenarios are shown to  
17 identify the source-receptor relationship. Finally, the results are summarized and future  
18 research directions are suggested in the conclusions.



1

## 2 **2. Method**

### 3 **2.1. Long-term surface observational data**

4 The hourly surface air quality monitoring data are obtained from the Airkorea website  
5 (<https://www.airkorea.or.kr>), including ozone (O<sub>3</sub>), NO<sub>2</sub>, SO<sub>2</sub>, CO, PM<sub>10</sub>, and PM<sub>2.5</sub> (PM<sub>2.5</sub>  
6 data are provided since 2015). As of March 2020, there are about 500 monitoring stations  
7 over South Korea. These routine monitor data are available for many decades and can serve  
8 as a main data set to examine long-term trends. We utilized hourly and daily maximum 8  
9 hour-average O<sub>3</sub> concentrations. O<sub>3</sub>, NO<sub>2</sub> and CO data are also averaged for spring and  
10 summer months. These surface monitoring data were used to investigate the impact of the  
11 COVID-19 pandemic in the Seoul Metropolitan area.

12

### 13 **2.2. Highway toll number and mobile phone usage data**

14 To examine changes in mobility pattern during the COVID-19 pandemic, traffic counts  
15 from the Korea Expressway Corporation daily transit data were used. The expressway  
16 transit data covering 2 years (2019 and 2020) of traffic passing toll gates were quantified  
17 from Hi-Pass (electronic toll collection system) and cash toll collection. Vehicles passing  
18 toll gates were not classified in details.



1

### 2 **2.3. Satellite data: tropospheric NO<sub>2</sub> columns**

3 We utilized the retrievals of the tropospheric NO<sub>2</sub> columns from the TROPOMI on board  
4 the Sentinel-5 Precursor (S5P) satellite. S5P satellite orbits on near polar sun-synchronous  
5 orbit with equator-crossing time of 13:30 local solar time (Veefkind et al., 2012).  
6 TROPOMI provides NO<sub>2</sub> column measurements at unprecedented fine spatial resolution  
7 of 5 km × 3.5 km (7 km × 3.5 km prior to 5 August 2019). Level 2 data with pixels  
8 passing quality assurance > 0.5 and the cloud fraction above 40% were selected for analysis.  
9 Much stricter recommendations provided by Sentinel-5 precursor TROPOMI Level 2  
10 product User Manual for nitrogen dioxide (Eskes et al., 2019) was not used in this analysis,  
11 to yield large enough number of sample sizes over aerosol-polluted regions. The  
12 TROPOMI data are regridded to a standard grid with a horizontal resolution of 0.1 latitude  
13 × 0.1 longitude (11 × 11 km) and monthly averaged values were derived. As the random  
14 error in the TROPOMI single-pixel uncertainties influence 40 to 60% of the tropospheric  
15 column abundance, temporal and spatial averaging may remove the random errors  
16 (Bauwens et al., 2020).

17

### 18 **2.4. CAM-Chem model simulations**



1 The atmospheric component of Community Earth System model (CESMv2.2), Community  
2 Atmosphere Model with Chemistry version 6 (CAM6-chem) is developed by National  
3 Center for Atmospheric Research (NCAR) (<https://www2.aocom.ucar.edu/gcm/cam-chem>).  
4 The CAM-chem adapted MOZART-T1 as the tropospheric chemistry mechanism  
5 (Emmons et al., 2010). The simulation used in this study was configured with 1° horizontal  
6 resolution. The sea surface temperature was prescribed, and meteorological fields were  
7 nudged to Modern-Era Retrospective analysis for Research and Applications version 2  
8 (MERRA-2) instead of using self-produced meteorological field  
9 (<https://gmao.gsfc.nasa.gov/reanalysis/MERRA-2/>). The simulation was performed from  
10 2000 to 2020 and applied CMIP6 emission inventory (2000-2014) and SSP5-8-5 emission  
11 inventory (2015-2020). The first 3 years were regarded as a spin-up. In this study, we  
12 utilized the CAM-Chem results to estimate the impact of stratospheric ozone on the surface  
13 in each season.

14

## 15 **2.5. WRF-Chem model simulations**

16 The Weather Research and Forecasting (WRF) model coupled with Chemistry (WRF-  
17 Chem) is developed by National Oceanic and Atmospheric Administration (NOAA) and  
18 National Center for Atmospheric Research (NCAR) and collaborating institutes (Grell et



1 al., 2005). We utilized WRF-Chem v4.4 to simulate regional meteorological fields and  
2 chemical compositions.

3 Our WRF-Chem set up utilizes the horizontal resolution of 28 x 28 km<sup>2</sup> and 60  
4 vertical levels. The simulation period is from 24th April 12 UTC to 11st June 12 UTC. We  
5 restart the simulation at 12 UTC every day to reduce computing errors. The first 7 days of  
6 model simulation is regarded as spin-up period. The analysis period is selected as 1st May  
7 to 10th June based on local time. The Global Forecast System (GFS) Final (FNL) analysis  
8 data are used for meteorological input and boundary conditions  
9 (<https://rda.ucar.edu/datasets/ds083.2/>). We used The Community Atmosphere Model with  
10 Chemistry (CAM-Chem) output to the chemical boundary and first initial conditions  
11 (<https://www.acom.ucar.edu/cam-chem/cam-chem.shtml>) (Buchholz et al., 2019). The  
12 Model of Emissions of Gases and Aerosols from Nature (MEGAN) is used for biogenic  
13 emissions (Guenther et al., 2006).

14 There are 7 model sensitivity runs that adopt different emission scenarios. The  
15 control run is based on the standard EDGAR-HTAPv2 emission inventory (Janssens-  
16 Maenhout et al., 2015). “No China” case removes all anthropogenic emissions in China.  
17 “No Seoul” case eliminates all anthropogenic emissions in Seoul. There is one case that  
18 decreased Chinese VOC emissions by 50%. There are two cases that reduced Chinese NO<sub>x</sub>



1 emissions by 50%: the one case has the same VOC emissions as in the control case while  
2 the other case has the 50% reductions of VOC emissions as well. Lastly, there is one case  
3 that reduced Chinese  $\text{NO}_x$  emissions by 75%. The WRF-Chem sensitivity runs are  
4 summarized in Section 4 (discussion section).

5

### 6 **3. Results**

7 In this study, ozone and its precursor concentrations in 7 cities, 9 provinces, and 3  
8 background sites in South Korea (Figure 1) are analyzed at diurnal, seasonal, and decadal  
9 time scales. Figure 2 shows the 4<sup>th</sup> highest daily maximum 8 hours-average ozone  
10 concentrations (MDA8  $\text{O}_3$ ) for the cities and provinces for ozone season (May-September)  
11 from 2001 to 2021. The 4<sup>th</sup> highest MDA8  $\text{O}_3$  increases by 1-2 ppb  $\text{yr}^{-1}$  for most of cities  
12 and provinces across South Korea in this period. The most of cities and provinces have the  
13 4<sup>th</sup> highest MDA8  $\text{O}_3$  higher than 70 ppb after 2010 (see gray dashed line in Figures 2 and  
14 3). The trend in Jeollanam-do is small and insignificant partly because the MDA8  $\text{O}_3$  was  
15 high before 2010. Widely increasing long-term ozone trends in South Korea indicate a  
16 regional nature of this pollutant, potentially influenced by Asian emissions, chemical  
17 transformations, and long-range transport. Therefore, it is imperative to understand the  
18 local and regional processes that enhance surface ozone. Ozone originated from Asia is  
19 known to be efficiently transported to North America during springtime (Jacob et al., 1999;  
20 Jaffe et al., 1999; Jaffe et al., 2003; Cooper et al., 2010; Lin et al., 2012; Langford et al.,



1 2017; Jaffe et al., 2018) and summertime (Fiore et al., 2002; Liang et al., 2007) as well.  
2 Investigating seasonal differences in ozone in South Korea may provide insights on the  
3 relative importance of local and regional processes. Table 1 summarizes the abundances  
4 and differences between spring and summer ozone concentrations averaged for the peak  
5 time (10-20 LT) and the base time (01-06 LT). For the base time, the ozone concentration  
6 in spring is always higher than that in summer: differences between the two seasons range  
7 from 3.1 to 14.5 ppb. This clearly indicates the importance of large-scale influences in  
8 spring. The results are the same for the peak time except for Seoul and Gyeonggi-do: the  
9 ozone concentrations in Seoul and Gyeonggi-do in summer are slightly higher than those  
10 in spring. The differences at the peak time are small for Incheon, Daegu, and  
11 Chungcheongbuk-do, suggesting the importance of local chemistry in the areas during  
12 summer.

13 Figure 4 shows the ratio of ozone exceedances in summer to those in spring for the  
14 cities, provinces, and background sites. There are more exceedances in summer than in  
15 spring in Seoul, Incheon, and Gyeonggi-do indicating that local summertime ozone  
16 production is important in these areas. In contrast, in the background sites such as Kosan,  
17 Gosung, and Ulleung-do, springtime exceedances dominate, which demonstrates the  
18 importance of high springtime ozone and its transport within Asia. For the rest of the  
19 regions, springtime and summertime exceedances are comparable or springtime  
20 exceedances are slightly higher than summertime counterparts. The same conclusions are



1 exhibited with diurnal variations of exceedances in Figure 5. Strongly enhanced  
2 summertime ozone exceedances are found during daytime from 13 to 20 LT, indicating  
3 efficient photochemical ozone production in this season. The peaks occurred at 17 LT in  
4 Seoul and Gyeonggi-do and one hour early at 16 LT in Incheon. Incheon is faced right to  
5 the West Sea (Figure 1). Thus, airmass flows from Incheon to Seoul under typical westerly  
6 or seabreeze condition. The late-afternoon peaks in the area (4-5 PM) and one hour late  
7 peak of exceedances in Seoul than Incheon suggest that local circulation plays an important  
8 role in a built-up and distribution of ozone within Incheon, Seoul, and Gyeonggi-do region.  
9 Springtime and summertime ozone exceedances mainly occur during daytime and night to  
10 some extents and the exceedances in the two seasons are similarly frequent in Daejeon,  
11 Pusan, and Daegu (Figure 5). It is interesting that the peaks in spring is about two hours  
12 later than those in summer for the three cities, indicating potential influence of transport in  
13 spring. Negligible exceedances from midnight to 10 LT in the three cities are due to high  
14  $\text{NO}_x$  pollution and depletion of ozone in association with  $\text{NO}_x$  at this time. In the  
15 background sites, springtime exceedances are much larger than summertime counterparts  
16 and nighttime exceedances are as frequent as daytime counterparts. In Gosung, springtime  
17 exceedances are about 20% all day long while summertime exceedances are less than or  
18 equal to 10% (Figure 5). The altitude of the observation site in Gosung is about 600 m  
19 above sea level. This location gives a unique opportunity to examine long-range transported  
20 plumes and background information at high altitude.



1           Stratospheric ozone can be deeply intruded in the low troposphere, elevating surface  
2 ozone during spring (Lin et al., 2012; Lin et al., 2015). It might be useful to understand the  
3 contribution of stratospheric ozone to surface in South Korea and its potential impacts on  
4 surface ozone trends in this region. Figure 6 shows the contribution of stratospheric ozone  
5 to the surface ozone in South Korea in each season. The stratospheric ozone influences the  
6 surface ozone in winter and spring most by 17-23 ppb from our global chemistry-climate  
7 model simulations. Approximately 37% (76%) of surface ozone in spring (winter)  
8 originated from stratosphere in South Korea according to the model (Table 2). In contrast,  
9 the influence of stratospheric ozone on the surface is minimum during summer, being about  
10 4% of the surface ozone concentration. Therefore, it would be beneficial to derive the ozone  
11 trends and exceedances independently in spring and summer. Meanwhile, it is noteworthy  
12 that the stratospheric ozone contribution to the surface ozone does not have clear trends  
13 during 2001-2021 (not shown).

14           In contrast to the trends of ozone, NO<sub>2</sub> and CO that are ozone precursors decreased  
15 both in spring and summer from 2001 to 2021 (Table 3). NO<sub>2</sub> reductions are the largest in  
16 Seoul, Pusan, Daegu, and Gyeongsangbuk-do, while CO reductions are evident for a wider  
17 region. The decreasing trends of NO<sub>2</sub> and CO are not significant in Ulsan throughout this  
18 period. Ozone increases in South Korea despite reduction of main precursors at local scale  
19 can be attributed to the increase of long-range transport of ozone or potentially “VOC-  
20 limited” (or “NO<sub>x</sub>-saturated”) local photochemical regime of South Korea. “VOC-limited”



1 regime is the condition in which  $\text{NO}_x$  (sum of  $\text{NO}$  and  $\text{NO}_2$ ) concentration is high and VOC  
2 is a limiting factor to form ozone. In this case, VOC reduction would decrease ozone, while  
3  $\text{NO}_x$  reduction would nonlinearly increase ozone. Since long-range transport from China  
4 is frequent during spring, it is useful to identify characteristics of ozone exceedance in  
5 spring separate from summer.

6 The frequency of springtime ozone exceedance increases from P1 (2002-2010) to P2  
7 (2011-2019) in all observation sites in South Korea (Figure 7). During COVID-19, however,  
8 the frequency of exceedances significantly decreases for most of the sites: large reductions  
9 occur in Daejeon, Daegu, Chungcheongbuk-do, Gyeongsangnam-do, Gyeongsangbuk-do,  
10 Gangwon-do as well as background sites such as Kosan (Cheju Island), Gosung (Gangwon-  
11 do), and Ulleung-do. Ozone exceedances decrease from 30% to 5% in Gosung from P2  
12 (2011-2019) to P3 (2020-2021) in spring. Gosung is close to the East Sea and is the farthest  
13 from China among the regions at a similar latitude range, but it is susceptible to long-range  
14 transported ozone because of its high elevation.  $\text{NO}_2$  concentration does not change much  
15 from P1 to P2 across all sites. On average, there was 5% decrease from P1 to P2. In contrast,  
16 during COVID-19 (from P2 to P3), there was 25% reductions of  $\text{NO}_2$  concentrations on  
17 average. CO concentrations also decreased by 22% from P1 to P2 and by 14% from P2 to  
18 P3. CO reductions are minor compared to  $\text{NO}_2$  changes during COVID-19. Decreases of  
19  $\text{O}_3$  exceedances during COVID-19 may be associated with  $\text{NO}_2$  decreases in this period. A  
20 notable feature is a large reduction of ozone in the background sites such as Kosan, Gosung,



1 and Ulleung-do, indicating cleaner background that may be affected by emission changes  
2 in Asian sources and long-range transport. Note that there were not significant NO<sub>2</sub> and CO  
3 concentration changes in the background sites from P2 to P3.

4 During summer, ozone exceedance frequencies also increase from P1 to P2 for all  
5 sites: Chungcheongnam-do has the largest increase from 3.2% to 11.3% and Gyeonggi-do,  
6 Daejeon, Jeollabuk-do, Gyeongsangnam-do and Gyeongsangbuk-do have similar increases  
7 (Figure 8). The ozone exceedances in the background sites Kosan, Gosung, and Ulleung-  
8 do also increase in this period. NO<sub>2</sub> and CO concentrations decreased marginally from P1  
9 to P2. During COVID-19, the ozone exceedance frequencies in summer increase in Seoul,  
10 Incheon, Gyeonggi-do, and Chungcheongnam-do, substantially decrease in Gangwon-do  
11 and the background sites, and remained at a similar level for the rest of sites. Because NO<sub>2</sub>  
12 concentrations decrease from P2 to P3 for Seoul, Incheon, Gyeonggi-do, and  
13 Chungcheongnam-do contrasting with increases of ozone exceedance, chemical regime for  
14 these regions during summer is likely to be VOC-limited (NO<sub>x</sub>-saturated) as mentioned  
15 above. Ozone exceedance substantially decreases in the background sites from P2 to P3,  
16 indicating cleaner air at large-scale. Figure 9 shows spatial distributions of TROPOMI  
17 tropospheric NO<sub>2</sub> columns in spring (MAM) and summer (JJA) in East Asia and their  
18 changes from 2019 to 2020 and from 2019 to 2021. The plot shows large reductions in NO<sub>2</sub>  
19 columns in spring in most of China and South Korea and surrounding seas during COVID-  
20 19. Figure 10 shows changes in traffic activities in the Seoul Metropolitan Area between



1 2019 and 2020. The number of cars counted at the highway tolls around this region  
2 decreased in March, April, and May in 2020 compared to 2019 by 6%. In June, this trend  
3 was reversed. The observed NO<sub>2</sub>, SO<sub>2</sub>, CO, PM<sub>10</sub>, and PM<sub>2.5</sub> concentrations were also  
4 reduced during spring in 2020 compared to 2019 by 10-30%. As in Figure 9, during summer,  
5 NO<sub>2</sub> columns also decrease in the same region, but with limited locations and less amounts  
6 compared to spring, during COVID-19. During spring, large reductions of NO<sub>2</sub> in China  
7 as observed by the satellite with or without reductions of VOC are likely to contribute to  
8 substantial decreases of ozone abundances in South Korea affected by long-range transport.  
9 Meanwhile, local NO<sub>x</sub> reductions in South Korea also can decrease ozone if NO<sub>x</sub> reductions  
10 are large enough in the presumably “VOC-limited” chemical regime in this area. The  
11 detailed source-receptor mechanism of ozone and its precursors in each season needs to be  
12 investigated further with long-term air quality model simulations in the future. In this study,  
13 the sensitivity of the ozone concentrations in Seoul and Gangwon-do to various emission  
14 scenarios in China and South Korea are discussed for a limited time period in the next  
15 section.

16

#### 17 **4. Discussions**

18 In this section, the WRF-Chem model simulations for the KORUS-AQ 2016 field  
19 campaign (mainly May, see Crawford et al., 2021 for details) are utilized to obtain insights  
20 about the impacts of emission changes on the ozone concentrations in Seoul and Gangwon-



1 do. In Figure 11, the vertical profiles of simulated ozone from various emission scenarios  
2 are shown. The two extreme cases are “No China” and “No Seoul” cases in which all  
3 anthropogenic emissions in China and Seoul are removed, respectively. Other cases are  
4 representing 50% Chinese NO<sub>x</sub> emission reduction only, 50% Chinese VOC emission  
5 reduction only, both Chinese NO<sub>x</sub> and VOC emission reductions by 50%, and 75% Chinese  
6 NO<sub>x</sub> emission reduction only scenarios. In Seoul, 50% Chinese NO<sub>x</sub> emission reduction  
7 only scenario slightly increases ozone concentration near the surface, but decreases it above  
8 500 m AGL (above ground level). 50% Chinese VOC emission reduction only scenario  
9 causes decrease of ozone concentration near the surface to 2000 m AGL. In the elevated  
10 layer (> 500-1000 m AGL) in Seoul, Chinese NO<sub>x</sub> emission reductions causes more  
11 decrease of ozone concentration than Chinese VOC emission reductions. Chinese NO<sub>x</sub> and  
12 VOC 50% emission reduction scenario led to decline of ozone concentrations near the  
13 surface to 2000 m AGL efficiently particularly above 1000 m AGL. 75% NO<sub>x</sub> emission  
14 reduction scenario decreased ozone concentration near the surface similar to both NO<sub>x</sub> and  
15 VOC 50% reduction scenario, but this case caused the largest ozone reductions above 1000  
16 m AGL except “No China” emission scenario. “No China” emission scenario led to 10-15  
17 ppb lower ozone concentrations in all altitudes than the control case. “No Seoul” emission  
18 scenario led to about 20 ppb higher ozone concentration than the control case partly  
19 because of much decreased ozone depletion reacting with NO. The sensitivity test results  
20 are similar for Seoul and Gangwon-do except that all emission scenarios (including “No



1 Seoul” and 50% Chinese NO<sub>x</sub> reduction scenarios) caused decline of ozone concentrations  
2 in Gangwon-do. Either NO<sub>x</sub> or VOC emission reductions in China clean air in Gangwon-  
3 do. The cleaning effect is largest above 500 m AGL. This may explain why the ozone  
4 exceedances sharply declined in Gosung, Gangwon-do located at ~650 m AGL during the  
5 COVID-19 pandemic (Figure 7). The sensitivity runs clearly demonstrate the long-range  
6 transport of Chinese ozone or the influence of Chinese emissions on the eastern part of  
7 Korean Peninsular such as Gangwon-do in May to beginning of June, 2016. Not only  
8 Chinese VOC emissions reductions but Chinese NO<sub>x</sub> emission reductions help to improve  
9 ozone pollution in the boundary layer (1-3 km) in South Korea.

10

## 11 **5. Summary and conclusions**

12 We investigated the spatiotemporal variability of surface ozone at 7 cities, 9 provinces, and  
13 3 background sites in South Korea from 2001 to 2021. The 4<sup>th</sup> highest MDA8 ozone  
14 concentrations increased for all cities, most of provinces and background sites for this  
15 period by 1-2 ppb yr<sup>-1</sup> and they were above 70 ppb approximately after 2010. Most of South  
16 Korean monitoring sites would have been non-attainment areas for the last decade if the  
17 US EPA National Ambient Air Quality Standards were applied.

18 The average ozone concentrations in spring were larger than those in summer at the  
19 base time (01-06 LT) for all observation sites (on average by 6.2 ppb). This was the same  
20 for the peak time (10-20 LT) except for Seoul and Gyeonggi-do in which the summer



1 average was about 1 ppb higher than the spring counterpart. The ozone concentrations in  
2 spring were on average 4.4 ppb larger than those in summer at the peak time. Higher mean  
3 ozone concentration in spring than summer can be associated with several factors. First,  
4 there are more influence of stratospheric ozone on the surface ozone in spring than summer.  
5 Our CAM-Chem simulations indicate that about 35% (5%) of surface ozone is attributed  
6 to stratospheric ozone in spring (summer). Another possibility is enhanced long-range  
7 transport of ozone from China in spring, which was not investigated systematically and  
8 statistically for multi-decadal time scales under a changing chemical and meteorological  
9 environment. A well-designed mathematical modeling approach would be helpful to  
10 disentangle multiple factors associated with background level, transport events, and  
11 chemical processes determining ozone in South Korea at a multi-decadal timescale.

12 Ozone exceedances in this study are defined as the ratio of the data with  
13 concentrations  $> 70$  ppb among all data, which is relevant to the US EPA standard. The  
14 ozone exceedances were more frequent in summer than spring in Seoul, Incheon, and  
15 Gyeonggi-do. The opposite was true for Jeollanam-do, Gyeongsangbuk-do, Gangwon-do,  
16 Chejudo, Ulleungdo, Daejeon, Gwangju, Kosan, and Gosung. For the rest of areas, the  
17 exceedance frequencies during spring and summer were similar. Ozone exceedances  
18 occurred most frequently at 16-19 LT (4-7 PM). However, ozone exceedances also occurred  
19 frequently during night at the background sites such as Kosan, Gosung, and Ulleungdo,  
20 indicating the possibility of strong influence of long-range transport on the surface ozone



1 level at these sites.

2 For precursors of ozone, the multi-decadal observations of NO<sub>2</sub> and CO in South  
3 Korea were analyzed. NO<sub>2</sub> concentrations showed overall declining trends, but significant  
4 and relatively large declinations were evident only in Seoul, Incheon, Gwangju, Pusan,  
5 Daegu, Gyeonggi-do, and Gyeongsangbuk-do ranging from -0.4 ppb yr<sup>-1</sup> (20-25%  
6 reductions for 21 yrs in SMA) to -0.8 ppb yr<sup>-1</sup> (-70% for 21 yrs in Gyeongsangbuk-do). CO  
7 concentrations also showed generally declining trends for most of sites with 13.9 ppb yr<sup>-1</sup>  
8 during spring and 8.9 ppb yr<sup>-1</sup> during summer. Current NO<sub>2</sub> (CO) concentration average  
9 was above 30 (400) ppb in SMA despite decrease of concentrations in the last two decades,  
10 still showing characteristics of highly polluted megacity. Other sites in South Korea also  
11 showed NO<sub>2</sub> (CO) concentration higher than 10 ppb (300 ppb) except for the background  
12 sites such as Kosan, Gosung, and Ulleungdo. VOCs are also essential ozone precursors.  
13 Ambient VOC concentrations were correlated with CO concentrations in the previous  
14 studies (Warneke et al., 2012). Therefore, high levels of CO concentration may indicate  
15 high levels of VOC concentration in South Korea. Unfortunately, multi-decadal VOC  
16 observations were not readily available for use in this study. Recent studies reported high  
17 level of aromatic and oxygenated VOC compounds in SMA during the KORUS-AQ 2016  
18 field campaign (Crawford et al., 2021). As with many megacities in the world, high ambient  
19 NO<sub>2</sub> concentration raises a possibility of “VOC-limited” chemical regime (or “NO<sub>x</sub>-  
20 saturated” in many areas of South Korea. Slight reduction of NO<sub>x</sub> (VOC) emissions would



1 increase (decrease) ozone concentration in this region. Another complication comes from  
2 long-range transport of ozone out of South Korea and its trends with time.

3 In this study, sensitivity tests of a regional chemical model to emission changes for a  
4 limited period were conducted, suggesting that Chinese NO<sub>x</sub> emissions reductions as well  
5 as VOC emission reductions help improve ozone pollution in South Korea. We also  
6 highlighted large reductions of ozone exceedances observed throughout all sites in South  
7 Korea in spring during the COVID-19 pandemic, with suppressed anthropogenic activities  
8 and consequently lower emissions both in China and South Korea. This hints the future  
9 direction to improve ozone pollution in South Korea and promotes further studies for  
10 projecting air quality and prioritizing actions for next decade or so.

11 In the future, multidecadal mathematical modeling at local to global scale as hindcast  
12 and forecast mode would be beneficial to better understand the trends of ozone in South  
13 Korea. Reliable VOC observations and intensive field campaigns similar to the KORUS-  
14 AQ 2016 would provide importance pieces to solve the puzzle of ozone in this area and  
15 help carefully monitor the changes in atmospheric composition relevant to ozone chemistry.

16

#### 17 **Code/Data availability**

18 The surface monitor data for South Korea can be downloaded from

19 <https://www.airkorea.or.kr/web/>. TROPOMI NO<sub>2</sub> columns are available at

20 <http://www.tropomi.eu/data-products/nitrogen-dioxide>. WRF-Chem model can be



1 downloaded from [https://www2.mmm.ucar.edu/wrf/users/download/get\\_sources.html](https://www2.mmm.ucar.edu/wrf/users/download/get_sources.html).

2 CAM-Chem (CESM) code is available at

3 [https://www.cesm.ucar.edu/models/cesm2/release\\_download.html](https://www.cesm.ucar.edu/models/cesm2/release_download.html).

4

#### 5 **Author contribution**

6 SWK initiates, designs, analyzes surface monitor data, and writes the manuscript, KMK,

7 SHS, and SWK design and conduct WRF-Chem model runs, JYJ, JYJ, and SWK design

8 and conduct CAM-Chem model runs, SHS processes the airkorea data, YSP and SHS

9 process, analyze, and visualize TROPOMI data, and YSP and JYJ collect and analyze the  
10 highway traffic data. All authors edit the manuscript.

11

#### 12 **Competing interests**

13 Authors declare no competing interests.

14

#### 15 **Acknowledgements**

16 This subject is also supported by the National Research Foundation of Korea (NRF) grant  
17 funded by the Korea government (MSIT) (No. 2020R1A2C2014131). The first author also  
18 acknowledges support from NRF-2018R1A5A1024958. KMA and KISTI supercomputing  
19 center support computing resources used (KSC-2021-RND-0040).



1 **References**

- 2 Bauwens M., et al. (2020), Impact of Coronavirus outbreak on NO<sub>2</sub> pollution assessed  
3 using TROPOMI and OMI observations, *Geophys. Res. Lett.*, 47 e2020GL.
- 4 Buchholz, R. R., Emmons, L. K., Tilmes, S., & The CESM2 Development Team (2019),  
5 CESM2.1/CAM-chem Instantaneous Output for Boundary Conditions. UCAR/NCAR  
6 - Atmospheric Chemistry Observations and Modeling Laboratory. Lat: -5 to 45, Lon:  
7 75 to 145, April 2016 – June 2016, Accessed 1 Oct 2019,  
8 <https://doi.org/10.5065/NMP7-EP60>.
- 9 Cooper, O., Parrish, D., Stohl, A., et al. (2010), Increasing springtime ozone mixing ratios  
10 in the free troposphere over western North America, *Nature*, 463, 344-348,  
11 <https://doi.org/10.1038/nature08708>.
- 12 Crawford, JH, Ahn, J-Y, Al-Saadi, J, Chang, L, Emmons, LK, Kim, J, Lee, G, Park, J-H,  
13 Park, RJ, Woo, JH, Song, C-K, Hong, J-H, Hong, Y-D, Lefer, BL, Lee, M, Lee, T, Kim,  
14 S, Min, K-E, Yum, SS, Shin, HJ, Kim, Y-W, Choi, J-S, Park, J-S, Szykman, JJ, Long,  
15 RW, Jordan, CE, Simpson, IJ, Fried, A, Dibb, JE, Cho, SY, Kim, YP (2021), The Korea–  
16 United States Air Quality (KORUS-AQ) field study. *Elementa: Science of the*  
17 *Anthropocene* 9(1). DOI: <https://doi.org/10.1525/elementa.2020.00163>.
- 18 Emmons, L. K., Schwantes, R. H., Orlando, J. J., Tyndall, G., Kinnison, D., Lamarque, J.-  
19 F., et al. (2020). The Chemistry Mechanism in the Community Earth System Model  
20 version 2 (CESM2). *Journal of Advances in Modeling Earth Systems*, 12,  
21 e2019MS001882. <https://doi.org/10.1029/2019MS001882>.
- 22 Eskes, H., J. van Geffen, F. Boersma, K.U. Eichmann, A. Apituley, M. Pedergnana, *et al.*  
23 (2019), Sentinel-5 precursor/TROPOMI level 2 product user manual nitrogen dioxide,  
24 Royal Netherlands Meteorological Institute, # S5P-KNMI-L2-0021-MA, issue 3.0.0,  
25 27.



- 1 Fiore, A. M., et al. (2002), Background ozone over the United States in summer: Origin,  
2 trend, and contribution to pollution episodes, *J. Geophys. Res.*, 107(D15), 4275,  
3 doi:10.1029/2001JD000982.
- 4 Gaudel, A., et al. (2018), Tropospheric ozone assessment report: present-day distribution  
5 and trends of tropospheric ozone relevant to climate and global atmospheric chemistry  
6 model evaluation, *Elem. Sci. Anthropocene*, 6:39, <https://doi.org/10.1525/elementa.291>.
- 7 Grell, G. A., S. E. Peckham, R. Schmitz, S. A. McKeen, G. Frost, W. C. Skamarock, and  
8 B. Eder, Fully coupled “online” chemistry within WRF model, *Atmos. Environ.*, 39(37),  
9 6957-6975, doi:10.1016/j.atmosenv.2005.04.027, 2005.
- 10 Guenther, A., Karl, T., Harley, P., Wiedinmyer, C., Palmer, P. I., and Geron, C. (2006),  
11 Estimates of global terrestrial isoprene emissions using MEGAN (Model of Emissions  
12 of Gases and Aerosols from Nature), *Atmos. Chem. Phys.*, 6, 3181–3210,  
13 <https://doi.org/10.5194/acp-6-3181-2006>.
- 14 Harkins, C., et al. (2021), A fuel-based method for updating mobile source emissions  
15 during the COVID-19 pandemic, *Environ. Res. Lett.* 16 065018.
- 16 Jacob, D. J., J. A. Logan, and P. P. Murti (1999), Effect of rising Asian emissions on surface  
17 ozone in the United States, *Geophys. Res. Lett.*, 26, 2175-2178,  
18 doi:10.1029/1999gl900450.
- 19 Jaffe, D., et al. (1999), Transport of Asian Air Pollution to North America, *Geophys. Res.*  
20 *Lett.*, 26, 711-714, doi:10.1029/1999GL900100.
- 21 Jaffe, D. A., et al. (2003), Increasing background ozone during spring on the west coast of  
22 North America, *Geophys. Res. Lett.*, 30, doi:10.1029/2003GL017024.
- 23 Jaffe, D. A., O. R. Cooper, A. M. Fiore, B. H. Henderson, G. S. Tonnesen, A. G. Russell,  
24 D. K. Henze, A. O. Langford, M. Lin, and T. Moore (2018), Scientific assessment of



1 background ozone over the U.S.: Implications for air quality management, *Elem. Sci.*  
2 *Anth.*, 6, 56, DOI:10.1525/elementa.309.

3 Janssens-Maenhout, G., Crippa, M., Guizzardi, D., Dentener, F., Muntean, M., Pouliot, G.,  
4 Keating, T., Zhang, Q., Kurokawa, J., Wankmüller, R., Denier van der Gon, H., Kuenen,  
5 J. J. P., Klimont, Z., Frost, G., Darras, S., Koffi, B., and Li, M. (2015), HTAP\_v2.2: a  
6 mosaic of regional and global emission grid maps for 2008 and 2010 to study  
7 hemispheric transport of air pollution, *Atmos. Chem. Phys.*, 15, 11411–11432,  
8 <https://doi.org/10.5194/acp-15-11411-2015>.

9 Kim, J., et al., (2018), Long-term trend analysis of Korean air quality and its implication  
10 to current air quality policy on ozone and PM<sub>10</sub>, *J. Korean Soc. Atmos. Environ.*, vol.  
11 34, no. 1, 1-15, <https://doi.org/10.5572/KOSAE.2018.34.1.001>.

12 Kim, Y. P., and G. W. Lee (2018), Trend of Air Quality in Seoul: Policy and Science,  
13 *Aerosol Air Qual. Res.*, 18, 2141-2156, <https://doi.org/10.4209/aaqr.2018.03.0081>.

14 Koo, J. H., et al. (2020), The implication of the air quality pattern in South Korea after the  
15 COVID-19 outbreak, *Scientific Reports*, 10:22462, [https://doi.org/10.1038/s41598-](https://doi.org/10.1038/s41598-020-80429-4)  
16 [020-80429-4](https://doi.org/10.1038/s41598-020-80429-4).

17 Korea Expressway Corporation transit data: Daily traffic counts using highway, available  
18 at: <http://data.ex.co.kr/portal/>, last access: 31 December 2020.

19 Lee, G. W., et al. (2020), Current status and future directions of tropospheric photochemical  
20 ozone studies in Korea, *J. Korean Soc. Atmos. Environ.*, vol. 36, no. 4, pp 419-441,  
21 doi:10.5572/KOSAE.2020.36.4.419.

22 Li, K., et al. (2019), Anthropogenic drivers of 2013-2017 trends in summer surface ozone  
23 in China, *P. Natl. Acad. Sci. USA*, 116, 2, 422-427,  
24 <https://doi.org/10.1073/pnas.1812168116>.



- 1 Li, K., et al. (2020), Increases in surface ozone pollution in China from 2013 to 2019:  
2 anthropogenic and meteorological influences, *Atmos. Chem. Phys.*, 20, 11423-11433,  
3 <https://doi.org/10.5194/acp-20-11423-2020>.
- 4 Liang, Q., et al. (2007), Summertime influence of Asian pollution in the free troposphere  
5 over North America, *J. Geophys. Res.*, 112, D12D11, doi:10.1029/2006JD007919.
- 6 Lin, M., et al. (2012), Transport of Asian ozone pollution into surface air over the western  
7 United States in spring, *J. Geophys. Res.*, 117, D00V07, doi:10.1029/2011JD016961.
- 8 Lin, M. Y., W. Horowitz, R. Payton, A. M. Fiore, G. Tonnesen: US surface ozone trends  
9 and extremes over 1980-2014 (2017), Quantifying the roles of rising Asian emissions,  
10 domestic controls, wildfires, and climate, *Atmos. Chem. Phys.*, 17(4), doi:10.5194/acp-  
11 17-2943-2017.
- 12 Lin, M. Y., L. W. Horowitz, Y. Xie, F. Paulot, S. Malyshev, E. Shevliakova et al. (2020),  
13 Vegetation feedbacks during drought exacerbate ozone air pollution extremes in Europe.  
14 *Nature Climate Change*, 10, 444-451.
- 15 Lu, X., et al. (2018), Severe surface ozone pollution in China: A global perspective, *Environ.*  
16 *Sci. Technol. Lett.*, 5, 487-494, <https://doi.org/10.1021/acs.estlett.8b00366>.
- 17 Lu, X., et al. (2020), Rapid increases in warm-season surface ozone and resulting health  
18 impact in China since 2013, *Environ. Sci. Tech. Lett.*, 7, 240-247,  
19 <https://doi.org/10.1021/acs.estlett.0c00171>.
- 20 National Research Council (1991), Rethinking the ozone problem in urban and regional air  
21 pollution, *National Academic Press*, 500pp.
- 22 Monks, P. S., Archibald, A. T., Colette, A., Cooper, O., Coyle, M., Derwent, R., Fowler, D.,  
23 Granier, C., Law, K. S., Mills, G. E., Stevenson, D. S., Tarasova, O., Thouret, V., von  
24 Schneidmesser, E., Sommariva, R., Wild, O., and Williams, M. L. (2015),



- 1 Tropospheric ozone and its precursors from the urban to the global scale from air  
2 quality to short-lived climate forcer, *Atmos. Chem. Phys.*, 15, 8889–8973,  
3 <https://doi.org/10.5194/acp-15-8889-2015>.
- 4 Seo, S., et al. (2021), Reductions in NO<sub>2</sub> concentrations in Seoul, South Korea detected  
5 from space and ground-based monitors prior to and during the COVID-19 pandemic,  
6 *Environ. Res. Commun.*, 3, 051005.
- 7 Veeffkind, J. P., Aben, I., McMullan, K., Förster, H., de Vries, J., Otter, G., Claas, J., Eskes,  
8 H. J., de Haan, J. F., Kleipool, Q., van Weele, M., Hasekamp, O., Hoogeveen, R.,  
9 Landgraf, J., Snel, R., Tol, P., Ingmann, P., Voors, R., Kruizinga, B., Vink, R., Visser,  
10 H., and Levelt, P. F. (2012), TROPOMI on the ESA Sentinel-5 Precursor: A GMES  
11 mission for global observations of the atmospheric composition for climate, air quality  
12 and ozone layer applications, *Remote Sens. Environ.*, 120, 70–  
13 83, <https://doi.org/10.1016/j.rse.2011.09.027>.
- 14 Warneke, C., J. A. deGouw, J. S. Holloway, J. Peischl, T. B. Ryerson, E. Atlas, D. Blake, M.  
15 Trainer, and D. D. Parrish (2012), Multiyear trends in volatile organic compounds in  
16 Los Angeles, California: Five decades of decreasing emissions, *J. Geophys. Res.*, 117,  
17 D00V17, doi:[10.1029/2012JD017899](https://doi.org/10.1029/2012JD017899).
- 18 Wang, W., et al. (2020), Exploring the drivers of the increased ozone production in Beijing  
19 in summertime during 2005-2016, *Atmos. Chem. Phys.*, 20, 15617-15633,  
20 <https://doi.org/10.5194/acp-20-15617-2020>.
- 21 Wang, W., et al. (2022), Long-term trend of ozone pollution in China during 2014-2020:  
22 distinct seasonal and spatial characteristics and ozone sensitivity, *Atmos. Chem. Phys.*,  
23 22, 8935-8949, <https://doi.org/10.5194/acp-22-8935-2022>.
- 24 Yeo, M. J., and Y. P. Kim (2021), Long-term trends of surface ozone in Korea, *Journal of*



1 *Cleaner Production*, 294, <https://doi.org/10.1016/j.jclepro.2020.125352>.

2



1 **List of Tables**

2

3 Table 1. Spring and summer ozone concentrations in Korean metropolitan cities and  
4 provinces. Both peak time (10-20 LT) and base time (01-06 LT) averages are shown.  
5 Differences in concentrations between spring and summer ( $O_3_{\text{spring}} - O_3_{\text{summer}}$ ) are in the  
6 parenthesis. The cities and provinces listed in the table are in counterclockwise order in  
7 regards to the South Korean map.

8

9 Table 2. Surface and stratospheric  $O_3$  concentrations and their ratio in Korea simulated by  
10 CESM. The concentrations and ratios for the altitude of 1 km are shown in parenthesis.

11

12 Table 3. The observed trends of  $NO_2$  and CO concentrations from linear fits of the data  
13 covering 2001-2021.

14

15

16



1 **Figure captions**

2

3 Figure 1. The locations of cities, provinces, and background sites in South Korea.

4

5 Figure 2. The trend of the 4<sup>th</sup> highest daily maximum 8 hours average (MDA8) O<sub>3</sub>  
6 concentrations in the South Korean metropolitan cities from 2001 to 2021. Only the data  
7 for May-September (ozone season) are used. Bars denotes standard deviations among the  
8 sites within the city. The slopes (S) and correlation coefficients (r) from linear fits are  
9 shown in parentheses. Grey dashed line indicates 70 ppb that is the air quality standard  
10 defined by the US Environmental Protection Agency.

11

12 Figure 3. The same as in Figure 2 except for South Korean provinces.

13

14 Figure 4. Ratio of O<sub>3</sub> exceedances in Summer to exceedances in Spring. The red line  
15 indicates an one to one line. X-axis denotes names of cities, provinces, and background  
16 sites. Cities - Seo (Seoul), Inc (Incheon), DaJ (Daejeon), Gwa (Gwangju), Pus (Pusan), Uls  
17 (Ulsan), DaG (Daegu); Provinces - Gye (Gyeonggi-do), ChB (Chungcheongbuk-do), ChN  
18 (Chungcheongnam-do), JeB (Jeollabuk-do), JeN (Jeollanam-do), Che (Cheju Island), GyN  
19 (Gyeongsangnam-do), GyB (Gyeongsangbuk-do), Gan (Gangwon-do); Background  
20 sites - Kos (Kosan, Cheju Island), Ull (Ulleung Island), and Gos (Gosung, Gangwon-do).  
21 The data for 2001-2019 are utilized.

22

23 Figure 5. Diurnal O<sub>3</sub> exceedances. (Top) Seoul, Incheon, Gyeonggi-do, (middle) Daejeon,  
24 Pusan, and Daegu, and (bottom) Kosan, Gosung, Ulleung Island (or Ulleungdo). The data



1 for 2001-2019 are utilized.

2

3 Figure 6. The contribution of stratospheric O<sub>3</sub> (O<sub>3s</sub>) to the O<sub>3</sub> concentrations in each season  
4 at surface and 1 km above ground level in South Korea.

5

6 Figure 7. (top) O<sub>3</sub> exceedances (%), (middle) NO<sub>2</sub> concentrations, and (bottom) CO  
7 concentrations in South Korean cities, provinces, and background sites during spring for  
8 2002-2010, 2011-2019, and 2020-2021 (COVID-19). X-axis denotes names of cities,  
9 provinces, and background sites. Cities - Seo (Seoul), Inc (Incheon), DaJ (Daejeon), Gwa  
10 (Gwangju), Pus (Pusan), Uls (Ulsan), DaG (Daegu); Provinces - Gye (Gyeonggi-do), ChB  
11 (Chungcheongbuk-do), ChN (Chungcheongnam-do), JeB (Jeollabuk-do), JeN (Jeollanam-  
12 do), Che (Cheju Island), GyN (Gyeongsangnam-do), GyB (Gyeongsangbuk-do), Gan  
13 (Gangwon-do); Background sites - Kos (Kosan, Cheju Island), Ull (Ulleung Island), and  
14 Gos (Gosung, Gangwon-do).

15

16 Figure 8. The same as Figure 7 except for summer.

17

18 Figure 9. Differences in TROPOMI tropospheric NO<sub>2</sub> columns between 2019 and 2020 or  
19 between 2019 and 2021 (Difference = NO<sub>2</sub> 2020 or 2021 - NO<sub>2</sub> 2019). Unit: molecules cm<sup>-2</sup>

20

21 Figure 10. (Top) the number of cars passing highway tolls near the Seoul Metropolitan  
22 Area (SMA) from January to June in 2019 and 2020, (bottom) difference (%) in the toll  
23 numbers, NO<sub>2</sub>, SO<sub>2</sub>, CO, PM<sub>10</sub>, and PM<sub>2.5</sub> concentrations in SMA during spring.

24



- 1 Figure 11. Vertical profiles of ozone from the WRF-Chem model simulations based on
- 2 various emission scenarios: (top) Seoul, and (bottom) Gangwon-do.
- 3



1 Table 1. Spring and summer ozone concentrations in Korean metropolitan cities and  
 2 provinces. Both peak time (10-20 LT) and base time (01-06 LT) averages are shown.  
 3 Differences in concentrations between spring and summer ( $O_3$  spring -  $O_3$  summer) are in the  
 4 parenthesis. The cities and provinces listed in the table are in counterclockwise order in  
 5 regards to the South Korean map.

Location		Peak time	Base time
		Spring / Summer (difference)	Spring / Summer (difference)
City	Seoul	34.4 / 35.6 (-1.2)	20.6 / 17.5 (3.1)
	Incheon	34.6 / 33.1 (1.5)	25.1 / 20.2 (4.9)
	Daejeon	41.2 / 37.0 (4.2)	22.8 / 19.1 (3.7)
	Gwangju	39.9 / 35.4 (4.5)	28.5 / 24.0 (4.5)
	Pusan	40.3 / 34.2 (6.1)	30.3 / 22.4 (7.9)
	Ulsan	38.7 / 33.4 (5.3)	25.8 / 18.7 (7.1)
	Daegu	39.6 / 37.6 (2.0)	24.0 / 19.6 (4.4)
Province	Gyeonggi-do	37.5 / 38.5 (-1.0)	20.8 / 18.0 (2.8)
	Chungcheongbuk-do	42.1 / 39.4 (2.7)	24.8 / 20.6 (4.2)
	Chungcheongnam-do	41.3 / 37.7 (3.6)	29.6 / 23.1 (6.5)
	Jeollabuk-do	38.3 / 35.0 (3.3)	26.7 / 23.6 (3.1)
	Jeollanam-do	42.5 / 35.1 (7.4)	33.0 / 24.1 (9.4)
	Cheju Island	49.0 / 35.0 (14.0)	43.7 / 29.2 (14.5)
	Gyeongsangnam-do	44.3 / 40.0 (4.3)	28.9 / 21.9 (7.0)
	Gyeongsangbuk-do	45.1 / 38.0 (7.1)	28.5 / 20.6 (7.9)
	Gangwon-do	45.6 / 39.5 (6.1)	31.5 / 24.0 (7.5)

6  
 7  
 8  
 9  
 10  
 11  
 12  
 13



1 Table 2. Surface and stratospheric O<sub>3</sub> concentrations and their ratio in Korea simulated by  
2 CESM. The concentrations and ratios for the altitude of 1 km are shown in parenthesis.

Season	Surface O <sub>3</sub>	Stratospheric O <sub>3</sub> (O <sub>3S</sub> )	Ratio (O <sub>3S</sub> /O <sub>3</sub> ) (%)
DJF	30.4 (46.2)	23.2 (26.4)	76.2 (57.2)
MAM	45.3 (64.2)	16.7 (21.4)	36.9 (33.3)
JJA	45.9 (53.9)	2.0 (3.0)	4.3 (5.6)
SON	36.3 (51.1)	9.8 (12.1)	26.9 (23.8)

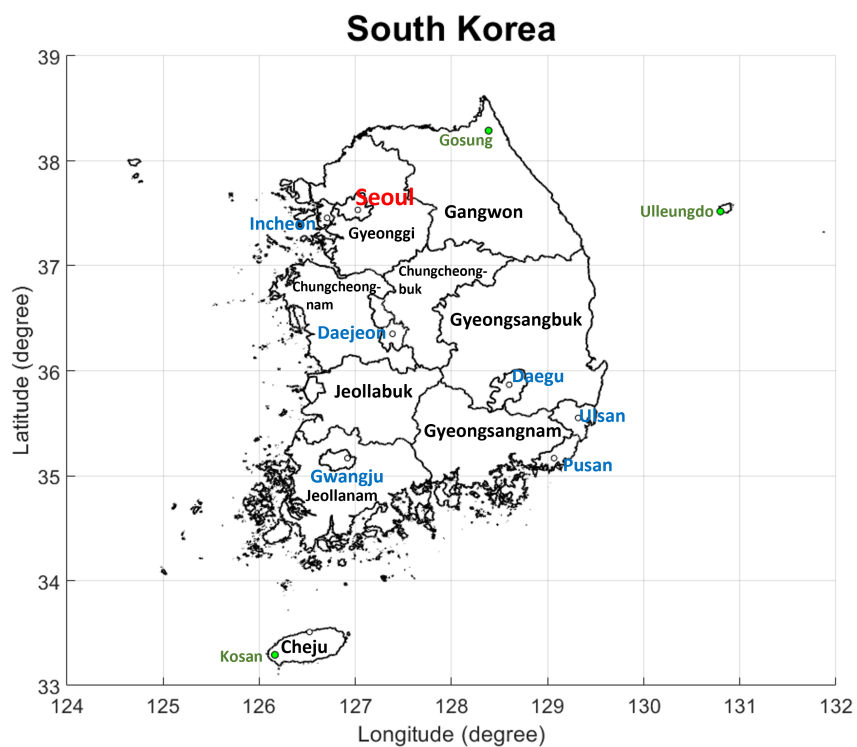
3  
4  
5  
6  
7  
8  
9  
10  
11  
12  
13  
14  
15  
16  
17  
18  
19  
20  
21  
22  
23



1 Table 3. The observed trends of NO<sub>2</sub> and CO concentrations from linear fits of the data  
 2 covering 2001-2021.

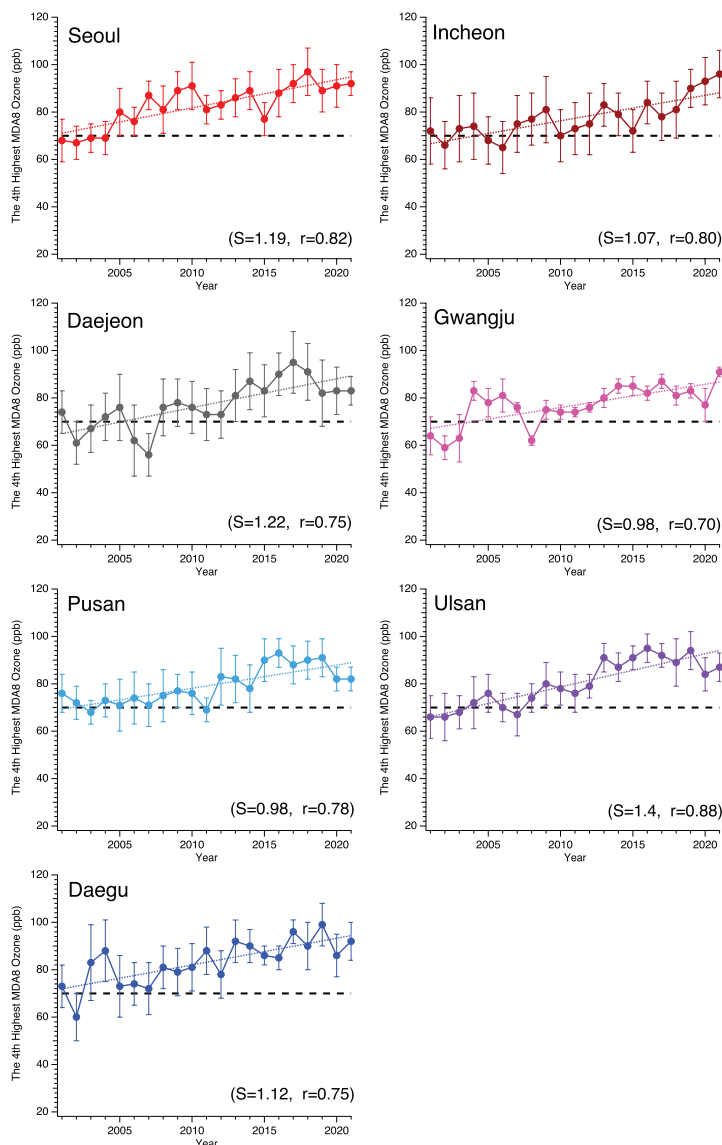
Stations		NO <sub>2</sub>	CO
		Spring / Summer Slope (Correlation Coefficient)	Spring / Summer Slope (Correlation Coefficient)
City	Seoul	-0.72 (-0.85)/-0.72(-0.91)	-7.56(-0.77)/-5.34(-0.83)
	Incheon	-0.37(-0.62)/-0.50(-0.62)	-7.65(-0.71)/-4.64(-0.66)
	Daejeon	-0.10(-0.29)/-0.12(-0.50)	-15.53(-0.79)/-9.71(-0.64)
	Gwangju	-0.51(-0.85)/-0.35(-0.88)	-10.64(-0.81)/-8.00(-0.69)
	Pusan	-0.64(-0.89)/-0.49(-0.90)	-12.32(-0.83)/-11.05(-0.81)
	Ulsan	-0.04(-0.08)/-0.06(-0.16)	-4.80(-0.39)/-0.75(0.07)
	Daegu	-0.65(-0.87)/-0.51(-0.89)	-23.49(-0.90)/-19.87(-0.87)
Province	Gyeonggi	-0.41(-0.66)/-0.44(-0.79)	-14.50(-0.95)/-8.82(-0.94)
	Chungcheongbuk	-0.18(0.39)/-0.16(-0.45)	-17.68(-0.78)/-6.49(-0.61)
	Chungcheongnam	-0.10(-0.30)/-0.12(-0.41)	-20.95(-0.76)/-9.33(-0.69)
	Jeollabuk	-0.17(-0.42)/-0.25(-0.65)	-21.33(-0.87)/-15.07(-0.85)
	Jeollanam	-0.21(-0.51)/-0.21(-0.58)	-5.86(-0.53)/-5.32(-0.48)
	Cheju	-0.18(-0.38)/-0.16(-0.46)	-10.74(-0.71)/-6.95(-0.50)
	Gyeongsangnam	-0.12(-0.31)/-0.10(-0.40)	-6.76(-0.58)/-3.92(-0.46)
	Gyeongsangbuk	-0.76(-0.89)/-0.49(-0.88)	-27.54(-0.82)/-17.48(-0.78)
	Gangwon	-0.16(-0.50)/-0.20(-0.69)	-15.31(-0.86)/-9.03(-0.71)

3  
 4  
 5  
 6  
 7  
 8  
 9



1  
2 Figure 1. The locations of cities, provinces, and background sites in South Korea.

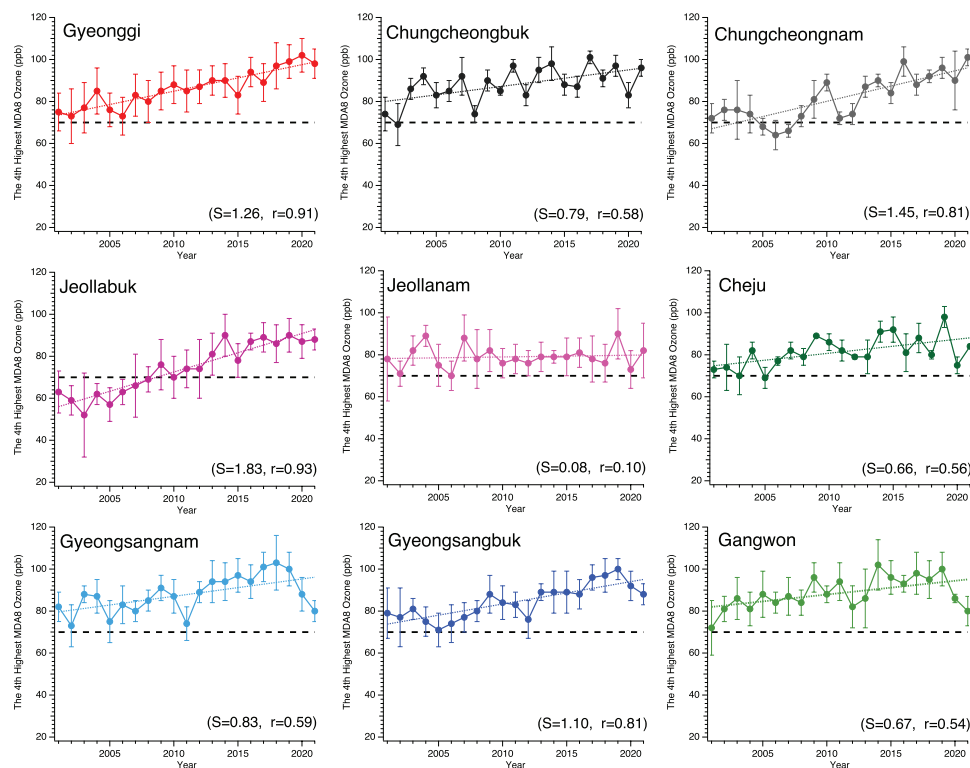
3  
4  
5  
6



1

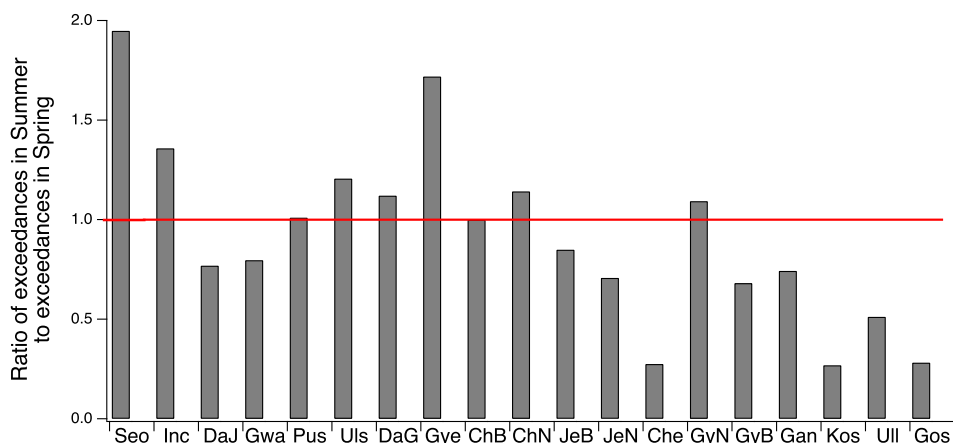
2 Figure 2. The trend of the 4<sup>th</sup> highest daily maximum 8 hours average (MDA8) O<sub>3</sub>  
3 concentrations in the South Korean metropolitan cities from 2001 to 2021. Only the data  
4 for May-September (ozone season) are used. Bars denote standard deviations among the  
5 sites within the city. The slopes (S) and correlation coefficients (r) from linear fits are  
6 shown in parentheses. Grey dashed line indicates 70 ppb that is the air quality standard  
7 defined by the US Environmental Protection Agency.

8



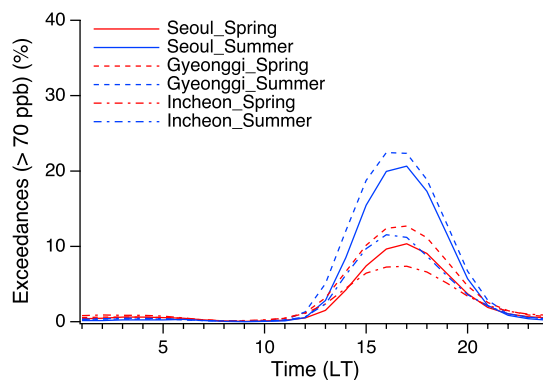
1  
2  
3  
4  
5  
6  
7  
8  
9  
10  
11  
12  
13  
14  
15  
16  
17  
18

Figure 3. The same as in Figure 2 except for South Korean provinces.

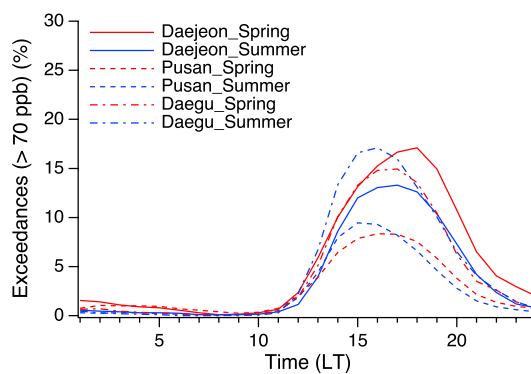


1  
2 Figure 4. Ratio of O<sub>3</sub> exceedances in summer to exceedances in spring. The red line  
3 indicates an one to one line. X-axis denotes names of cities, provinces, and background  
4 sites. Cities - Seo (Seoul), Inc (Incheon), DaJ (Daejeon), Gwa (Gwangju), Pus (Pusan), Uls  
5 (Ulsan), DaG (Daegu); Provinces - Gye (Gyeonggi-do), ChB (Chungcheongbuk-do), ChN  
6 (Chungcheongnam-do), JeB (Jeollabuk-do), JeN (Jeollanam-do), Che (Cheju Island), GyN  
7 (Gyeongsangnam-do), GyB (Gyeongsangbuk-do), Gan (Gangwon-do); Background  
8 sites - Kos (Kosan, Cheju Island), Ull (Ulleung Island), and Gos (Gosung, Gangwon-do).  
9 The data for 2001-2019 are utilized.

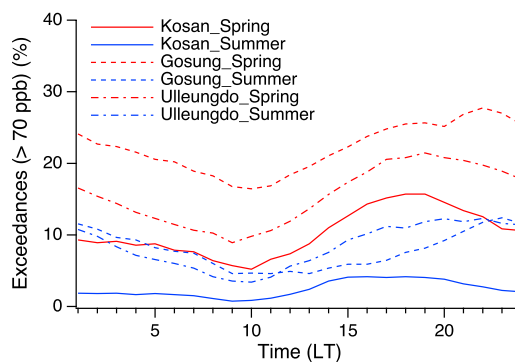
10  
11  
12  
13  
14  
15  
16  
17  
18  
19  
20  
21  
22  
23  
24  
25



1



2



3

4 Figure 5. Diurnal O<sub>3</sub> exceedances. (Top) Seoul, Incheon, Gyeonggi-do, (middle) Daejeon,  
5 Pusan, and Daegu, (bottom) Kosan, Gosung, Ulleung Island (or Ulleungdo). The data for  
6 2001-2019 are utilized.

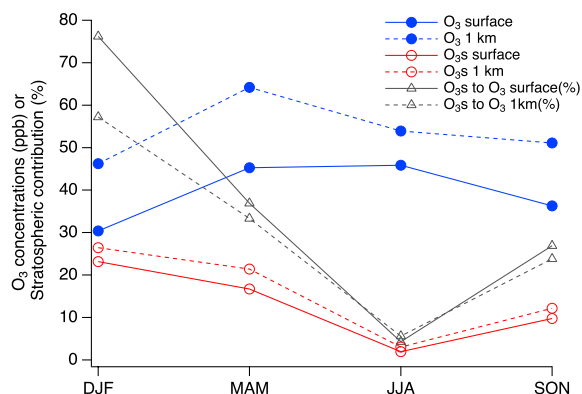
7

8

9

10

11



1

2 Figure 6. The contribution of stratospheric O<sub>3</sub> (O<sub>3s</sub>) to the O<sub>3</sub> concentrations in each season  
3 at surface and 1 km above ground level in South Korea. The plotted values are extracted  
4 from the CESMv2.2 results.

5

6

7

8

9

10

11

12

13

14

15

16

17

18

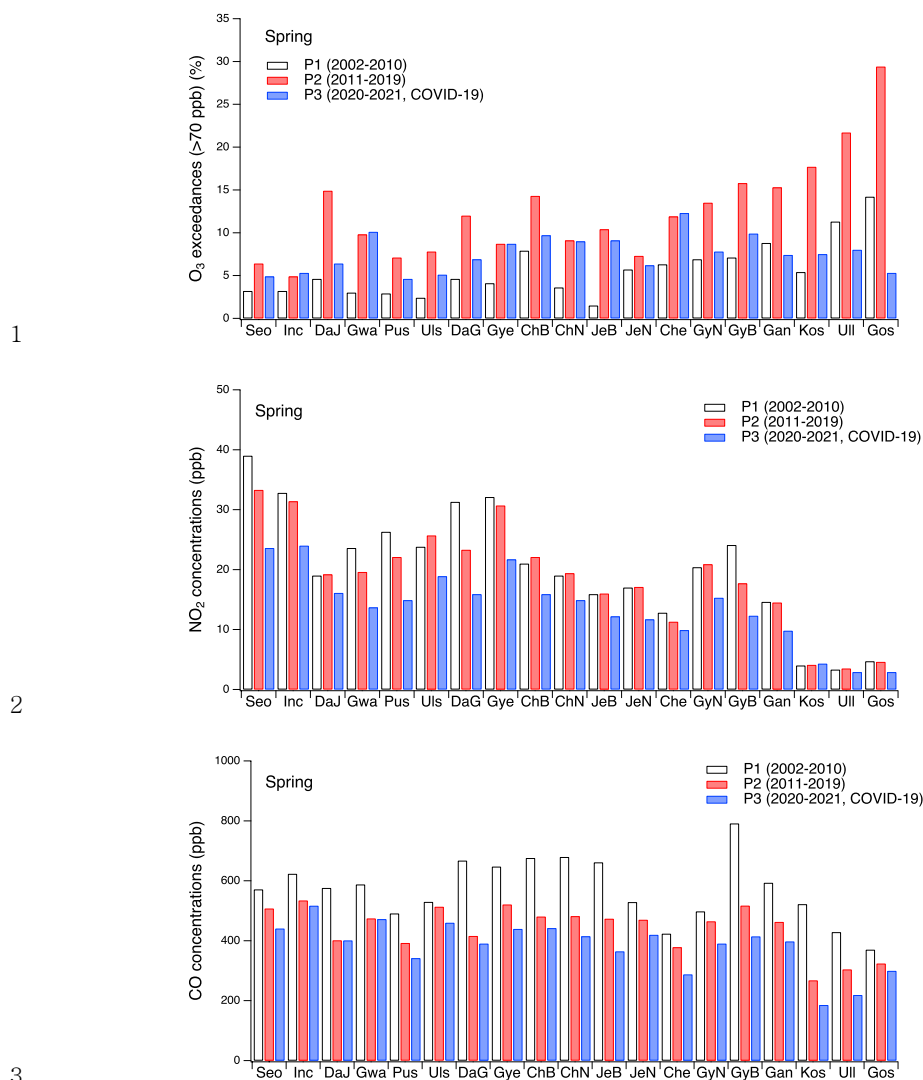
19

20

21

22

23



4 Figure 7. (Top) O<sub>3</sub> exceedances (%), (middle) NO<sub>2</sub>, and (bottom) CO concentrations in  
5 South Korean cities, provinces, and background sites during spring for 2002-2010, 2011-  
6 2019, and 2020-2021 (COVID-19). X-axis denotes names of cities, provinces, and  
7 background sites. Cities - Seo (Seoul), Inc (Incheon), DaJ (Daejeon), Gwa (Gwangju), Pus  
8 (Pusan), Uls (Ulsan), DaG (Daegu); Provinces - Gye (Gyeonggi-do), ChB  
9 (Chungcheongbuk-do), ChN (Chungcheongnam-do), JeB (Jeollabuk-do), JeN (Jeollanam-  
10 do), Che (Cheju Island), GyN (Gyeongsangnam-do), GyB (Gyeongsangbuk-do), Gan  
11 (Gangwon-do); Background sites - Kos (Kosan, Cheju Island), Ull (Ulleung Island), and  
12 Gos (Gosung, Gangwon-do).

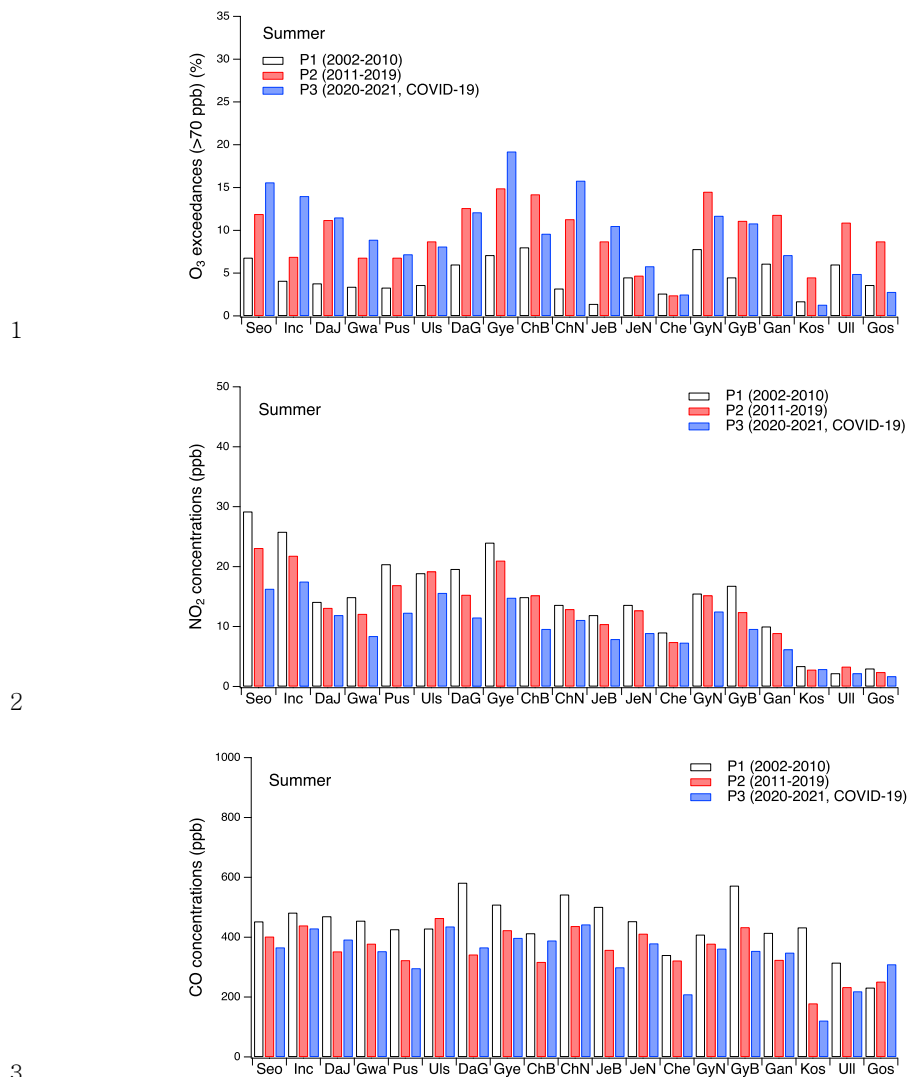
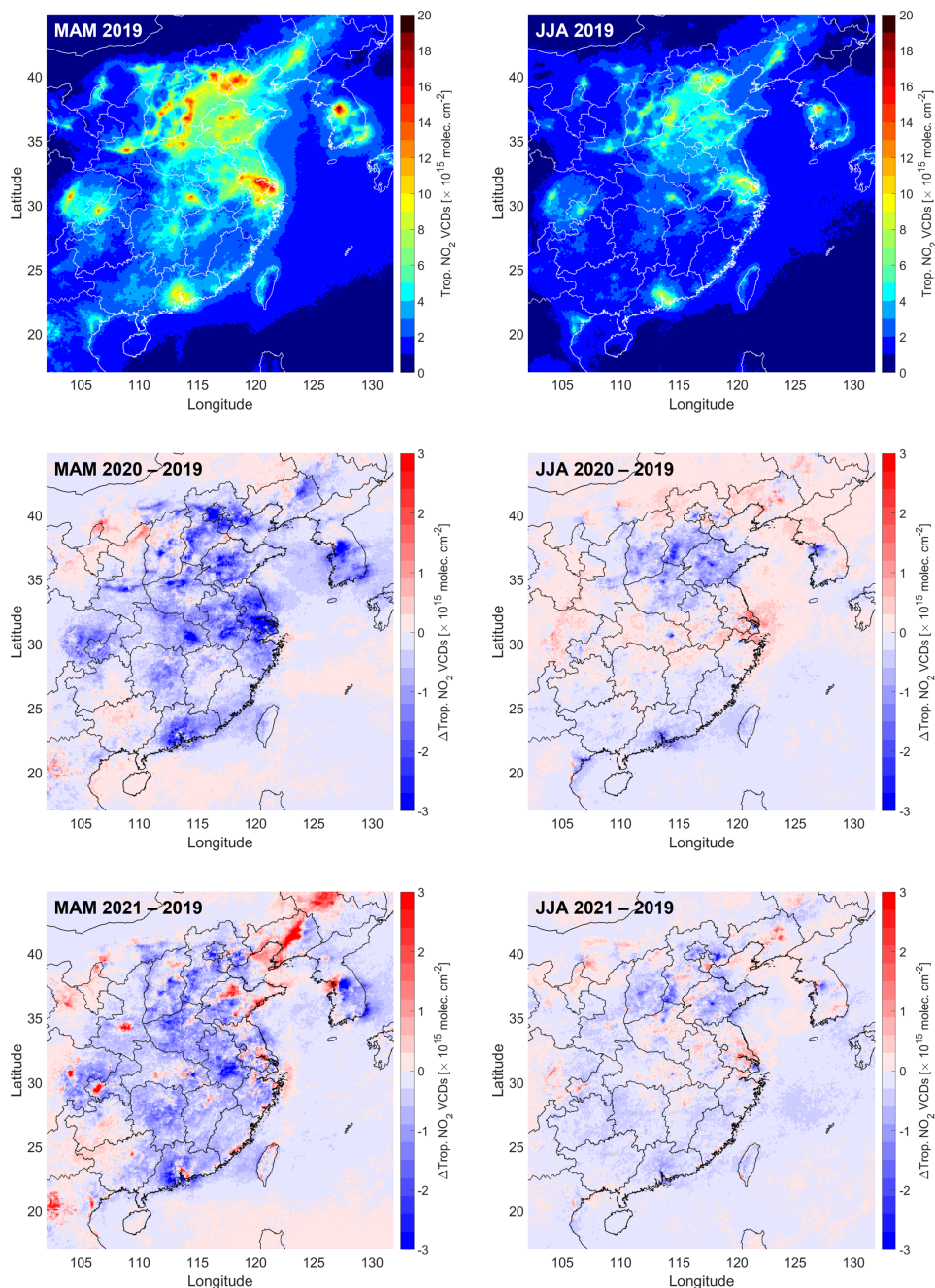


Figure 8. The same as Figure 7 except for summer.

4

5

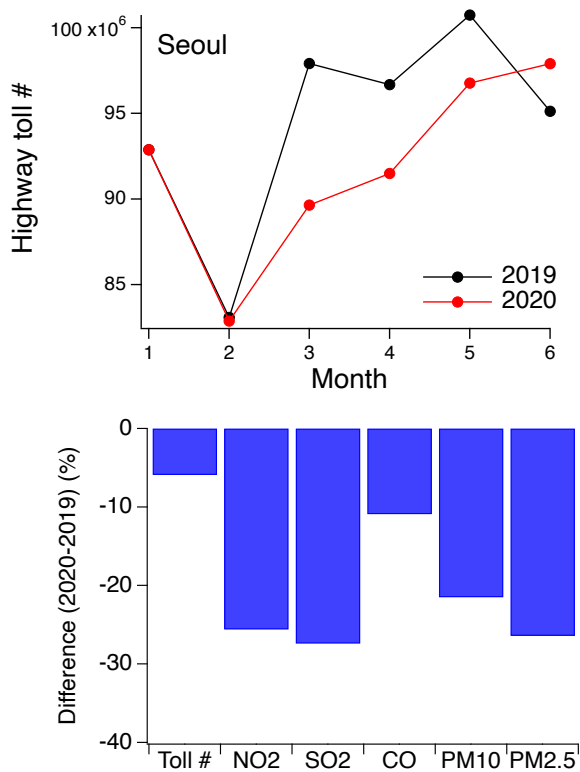
6



1

2 Figure 9. Differences in TROPOMI tropospheric NO<sub>2</sub> columns between 2019 and 2020 or  
3 between 2019 and 2021 (Difference = NO<sub>2</sub> 2020 or 2021 - NO<sub>2</sub> 2019). Unit: molecules cm<sup>-2</sup>

4



1

2

3 Figure 10. (Top) the number of cars passing highway tolls near the Seoul Metropolitan  
4 Area (SMA) from January to June in 2019 and 2020, (bottom) difference (%) in the toll  
5 numbers, NO<sub>2</sub>, SO<sub>2</sub>, CO, PM<sub>10</sub>, and PM<sub>2.5</sub> concentrations in SMA during spring.

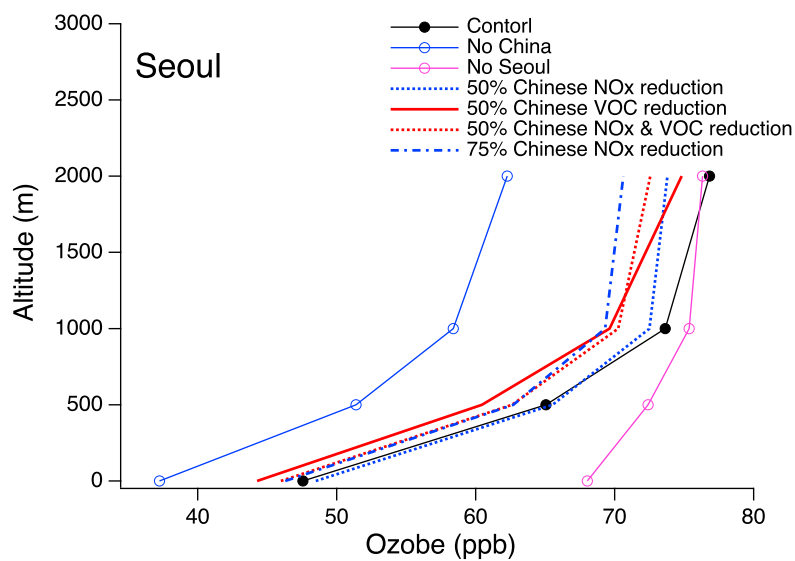
6

7

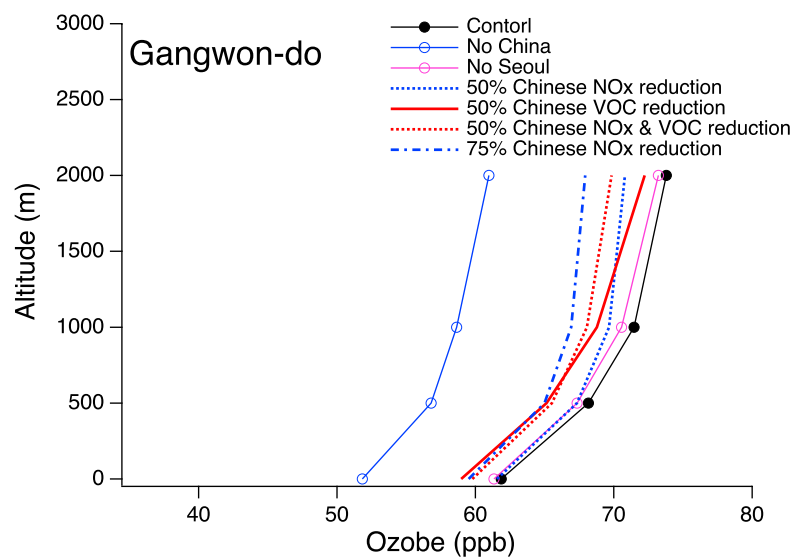
8

9

10



1



2

3

4 Figure 11. Vertical profiles of ozone from the WRF-Chem model simulations based on  
5 various emission scenarios: (top) Seoul, and (bottom) Gangwon-do.

6